

# LAY-UP OPTIMISATION OF COMPOSITE PLATES TO DELAY MODE-JUMP INSTABILITIES

B.G. Falzon\*<sup>1</sup>, A. Faggiani\* D. Brunner\*\*

\*Department of Mechanical & Aerospace Engineering, Monash University, VIC, 3800, Australia.

\*\*ETH Swiss Federal Institute of Technology, CH-8092 Zurich, Switzerland

<sup>1</sup>Brian.Falzon@monash.edu

**Keywords:** carbon fibre composites, optimisation, mode-jumping, genetic algorithms

## Abstract

*Experimental and numerical studies have shown that the occurrence of abrupt secondary instabilities, or mode-jumps, in a postbuckling stiffened composite panel may initiate structural failure. This study presents an optimisation methodology, using a genetic algorithm and finite element analysis for the lay-up optimisation of postbuckling composite plates to delay the onset of mode-jump instabilities. A simple and novel approach for detecting mode-jumps is proposed, based on the RMS value of out-of-plane pseudo-velocities at a number of locations distributed over the postbuckling structure.*

## 1 Introduction

Various studies have shown that compressively-loaded thin-skinned stiffened composite panels are able to sustain load in a postbuckled state [1-3], enabling the design of very lightweight aircraft structures. Experimental and theoretical investigations have further shown that these panels often undergo abrupt secondary instabilities, also referred to as ‘mode-jumps’, which may initiate catastrophic failure [4]. This paper builds on the earlier work by the first two authors, where an optimisation strategy was presented for the lay-up optimisation of a composite stiffened panel to delay the onset of skin-stiffener debonding [5] which often leads to catastrophic failure. A consequence of that study was the observation that the optimised panel exhibited a delayed secondary instability. This was consistent with the hypothesis that

secondary instabilities may trigger failure and therefore by delaying this event, ultimate structural failure is also delayed.

An optimisation strategy, using a Genetic Algorithm linked to a Finite Element Analysis package, was developed where the objective function was based on maximising the load at which a secondary instability occurred. An efficient and effective means of detecting the onset of this highly non-linear event was based on tracking the rate of change in the out-of-plane displacement with respect to applied loading (pseudo-velocity), recorded at a number of sampling nodes in the finite element model. The root mean square (RMS) of all these values was then calculated to yield a representative metric indicating the onset of structural instability.

## 2 Finite element model

A composite plate with clamped boundary conditions and loaded in uniaxial compression, was modelled to demonstrate the optimisation methodology. The dimensions and baseline lay-up are given in Fig. 1. The edges were clamped to induce high membrane stresses which are known to promote mode-jumping [6]. General-purpose shell elements with reduced integration (SR4), each with four nodes and six degrees of freedom at each node, were used in the finite element package ABAQUS/Standard [7]. Each element contained three integration points per ply through the thickness. Material properties, corresponding to an average of the tensile and

compressive values shown in Table 1 were used. Fig. 1 shows the final model for the plate and its associated mesh. Various sampling point locations on the plate were selected to measure the pseudo-velocities. These points had a longitudinal separation of 91 mm and 46 mm in the width direction, with point 11 corresponding to the centre of the plate

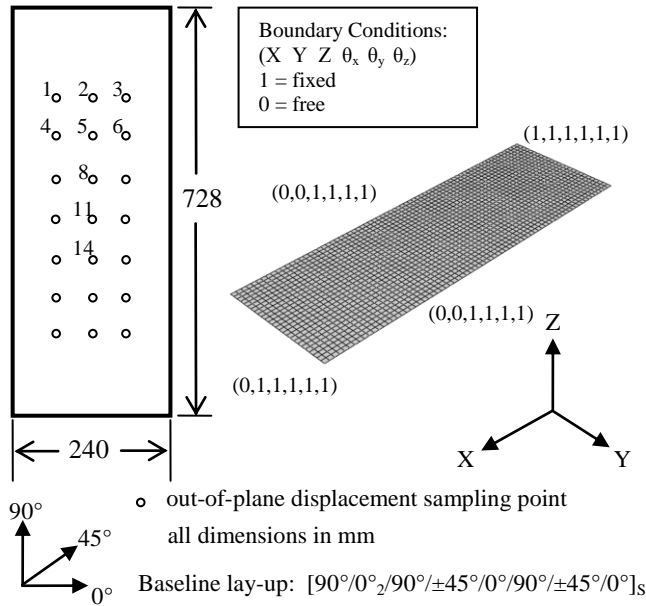


Fig.1: Finite element model of composite plate.

Table 1: Material properties for T800/924C.

Property	Value
$E_{11tension}$	162 GPa
$E_{11compression}$	145 GPa
$E_{22tension}$	9.2 GPa
$E_{22compression}$	9.5 GPa
$G$	5.0 GPa
$\nu$	0.3
$t$	0.125 mm

### 3 Modelling validation

A linear buckling eigenvalue analysis was conducted to extract the first two mode-shapes. These were used to introduce an imperfection in the flat plate, corresponding to a linear combination of these two mode-shapes with a maximum out-of-plane imperfection of 2% of the skin thickness (2.75mm). This was followed by a non-linear analysis of the baseline design,

in ABAQUS/Standard where damping forces were introduced to stabilize the solution. This plate had a lay-up and dimensions which were identical to the central skin-bay of a composite stiffened panel which was tested to failure as part of a previous research program [8]. Since the bounding stiffeners provided a boundary condition which closely resembled the clamped conditions on the flat plate, the qualitative initial and secondary (mode-jump) buckling mode shapes, obtained from the finite element analysis, was in good agreement with those observed experimentally, Fig. 2.

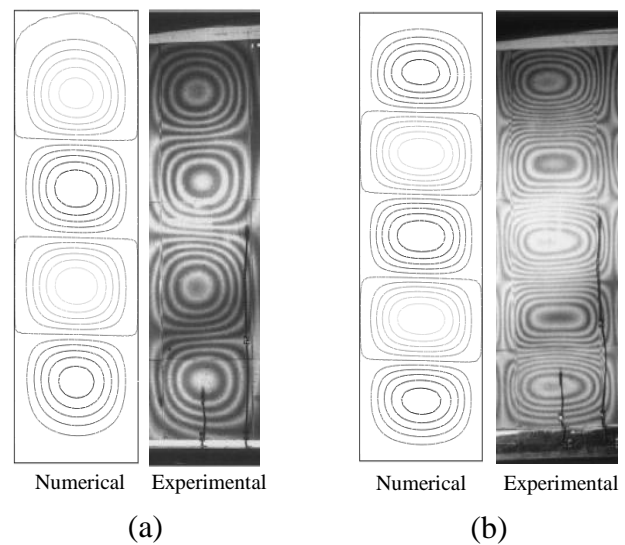


Fig.2: Numerical and experimental (Moire fringes) out-of-plane displacement contours just after (a) buckling and (b) mode-jump.

### 4 Capturing the onset of mode-jumping

A central objective of this study was to develop an efficient means of detecting the onset of secondary instabilities which could be easily incorporated in an objective (or fitness) function within a Genetic Algorithm. While a number of methods are available; for example, by detecting changes in the sign of the entries in the diagonal matrix of a factored assembled stiffness matrix [9], it is not always possible to extract such information from commercial finite element packages.

Extensive observations have confirmed that a secondary instability tends to occur rapidly,

often within milliseconds [4]. Under a displacement-controlled quasi-static simulation, rapid changes in deflections are observed for a small increment in loading. It is this latter phenomenon which is exploited for detecting secondary instabilities. A number of sample points (at pre-determined finite element nodes) were selected over the surface of the plate as shown in Fig. 1.

Throughout the nonlinear analysis, the change in out-of-plane displacement at these sampling points was recorded to obtain a measure of the out-of-plane pseudo-velocity,  $\Delta u_3^{t+\Delta t} / \Delta t$ , for each point at each increment.  $\Delta t$  refers to the increment in pseudo-time. The root mean square (RMS) of all values was then calculated to obtain a representative metric to indicate a structural instability:

$$RMS^{t+\Delta t} = \sqrt{\frac{\sum_{k=1}^n \left( \frac{\Delta u_3^{t+\Delta t}}{\Delta t} \right)_k^2}{n}} \quad (1)$$

where  $n$  is the number of sampling points used. A plot of the  $RMS^{t+\Delta t}$  function evaluations for the developed finite element model of the baseline design is given in Fig. 3 and shows that local maxima occurred at the onset of structural instabilities. A first local maximum is evident at the buckling point. A much larger increase in the  $RMS$  metric occurred at the onset of the secondary instability associated with the mode jump from four half-waves to five half-waves.

## 5 Genetic Algorithm

The aim of the optimisation routine was to delay the onset of secondary instabilities and a natural choice of an appropriate fitness function was one which directly used the secondary instability load and penalized those designs which underwent mode-jumping at relatively lower compression loading. The design variables were the ply orientations, restricted to take the values of  $0^\circ$ ,  $45^\circ$ ,  $-45^\circ$ , and  $90^\circ$ ,

commonly used in industry. Since the lay-up was assumed to be symmetric, each design ‘chromosome string’ had 11 ‘genes’, where each gene was expressed as either 1( $0^\circ$ ), 2( $90^\circ$ ), 3( $45^\circ$ ) or 4( $-45^\circ$ ). Constraints were also imposed on the initial buckling load

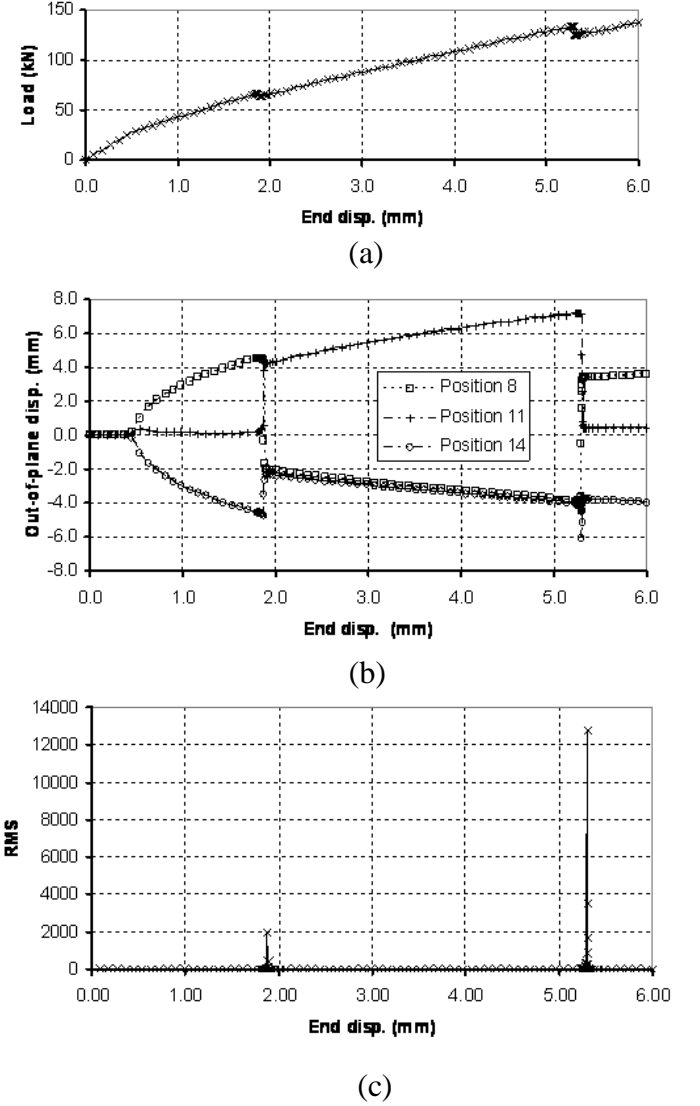


**Fig.3:** Results of finite element model of baseline design (a) load versus end-displacement curve (b) out-of-plane displacements (c) RMS function from Eq. 1.

and pre-buckling stiffness which were not allowed to reduce by more than 10% of those obtained from the baseline design. An additional constraint was set to prevent individual designs from having more than two contiguous plies at the same orientation as this can potentially promote matrix cracking [10].

A fixed population of 60 possible designs was chosen, with the initial population being randomly generated. Linear eigenvalue analysis was conducted to extract the initial buckling mode shapes to be used for introducing initial imperfections for the subsequent non-linear finite element analysis. The RMS function (Eq. 1) was used to detect initial buckling and mode-jumping. Individuals violating the buckling load and pre-buckling stiffness design constraints were ‘penalised’ prior to ranking this initial population according to a fitness function which related directly to the magnitude of the secondary instability load.

The fundamental concept behind Genetic Algorithms is the successive evolution of new generations based on ‘selective breeding’. Individuals from the initial and subsequent generations were selected using stochastic universal sampling [11]. Selected individuals were then ‘bred’ by the Genetic Algorithm using ‘two-point crossover’ where two randomly placed cut-off points are made in each individual/chromosome and then swapping information between two individuals to create new offspring, as shown in Table 2.

**Table 2:** Two-point crossover genetic operator

Parents	Offspring
24/31141/2441	24/14332/2441
12/14332/2132	12/31141/213

Following crossover, ‘mutation’ was applied to prevent the loss of potentially favourable genetic traits. This mutation was assigned a very low probability of occurring. Mutation acts by changing a random bit in a chromosome string and thus acts as a safety net to recover good genetic material which may have been lost during selection and crossover. Following mutation, a fitness based re-insertion scheme was used so that the generated offspring directly replaced the least fit individuals in the population. This method tends to preserve attractive genetic traits, hence aiding in achieving convergence in a reduced number of

generations. The whole genetic process was repeated until the GA found the optimum lay-up for the plate to delay the onset of secondary instabilities. A termination scheme was applied so that if five successive individuals in the population had the same chromosome string, then this chromosome string was deemed as the optimum. As a safety measure, a maximum number of 100 generations was also set.

## 6 Results

The Genetic Algorithm was developed in MATLAB and linked to ABAQUS for the finite element analysis. For this particular study, convergence was achieved after 53 generations. Fig. 4 shows the normalized median objective function for each generation plotted against the generation number. It is noted that at convergence, most individuals in the population had an optimum lay-up and consequently a high median value of the objective function

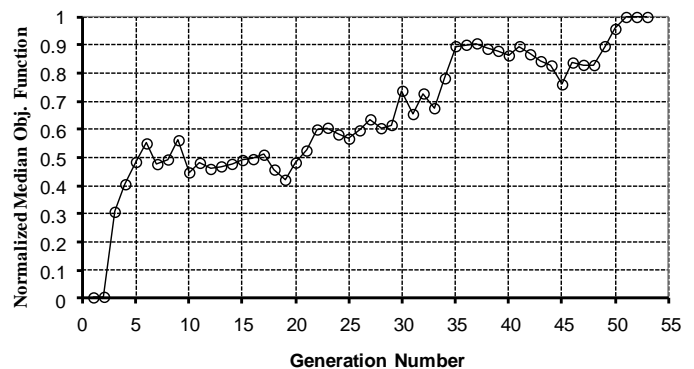


**Fig.4:** Normalised median objective function plotted against generation number.

The Genetic Algorithm evolved an optimum skin lay-up of  $[0/90/-45/90/45/90_2/-45/90/-45/90]_s$ . Table 3 compares the optimum configuration with the original, baseline plate lay-up. A linear buckling analysis predicted a buckling load for the optimised lay-up of 32.3 kN, 10.6% higher than the 29.2 kN value for the original baseline design. The pre-buckling stiffness of the optimum design was 89.3 kN, 58.9 % higher than that of the non-optimised design. The Genetic Algorithm was hence able to find an optimum solution not only within the bounds of the constraints imposed on the

optimisation – a maximum of 10% reduction in buckling load and pre-buckling stiffness as compared to the original baseline skin bay model – but in fact yielded an optimum design with superior buckling load and stiffness where a secondary instability was delayed to a load of 119.8 kN compared to the non-optimised value of 66.7 kN.

configuration. Fig. 7 shows numerically recorded out-of-plane displacements at the same positions on the plate as was shown in Fig. 3(b) for the non-optimised panel. The occurrence of buckling is marked by a rapid increase in out-of-plane displacement values, and evidence of a secondary instability and associated mode-jump is clearly visible via the sudden change in out-

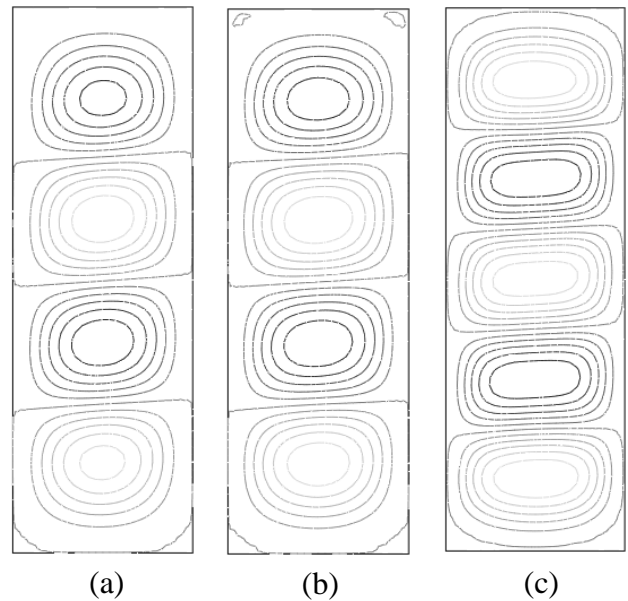
**Table 3:** Optimisation results

	Non-optimised	Optimised	% difference
Panel layup	[90/0 <sub>2</sub> /90/±45/0/90/±45/0] <sub>s</sub>	[0/90/-45/90/45/90 <sub>2</sub> /-45/90/-45/90] <sub>s</sub>	
Buckling load, kN	29.2	32.3	+10.6 %
Prebuckling stiffness, kN/mm	56.2	89.3	+58.9 %
Onset of secondary instability, kN	66.7	119.8	+79.6 %

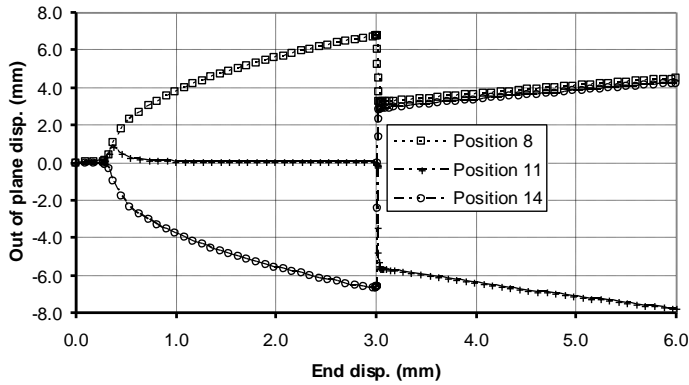
The mode shapes corresponding to the first two eigenvalues for the optimised plate were very similar to those of the non-optimised design shown in Fig. 2. The behaviour of the optimised design, as predicted by the ABAQUS nonlinear solver, is shown in Fig. 5 in terms of out-of-plane displacement contours, which may be compared with Fig. 2 for the non-optimised plate. Similarly to the non-optimised plate, the optimised design buckled into a four half-wave configuration as shown in Fig. 5(a), but at the higher buckling load of 32.3 kN, compared to 29.2 kN. As the loading was increased, the non-optimised plate mode-jumped to a five half-wave configuration at a loading of 66.7 kN, whilst the optimised plate maintained its four half-wave configuration, Fig. 5(b). A secondary instability in the optimised plate developed at the higher loading of 119.8 kN, also corresponding to a sudden mode-jump from four to five half-wavelengths, shown in Fig. 5 (c).

Fig. 6 shows the load displacement curve for the optimal lay-up. The load-displacement curve of the baseline plate, as in Fig. 3(a), is also shown for comparative purposes. It can be seen that the optimised design shows a greater buckling load and pre-buckling stiffness, and evidence of the mode-jump from four to five half-waves can be seen as a slight load drop in the load-displacement curve which occurs at a substantially higher loading for the optimised

of-plane displacement measurements as was discussed for the case of the non-optimised plate.



**Fig.5:** Out-of-plane displacement contours for the optimized skin bay lay-up just after (a) buckling (b) at a loading of 66.7 kN (c) after mode-jump at 108.6 kN.



**Fig.6:** Numerical load vs end-displacement curves for optimized and non-optimized composite plates.

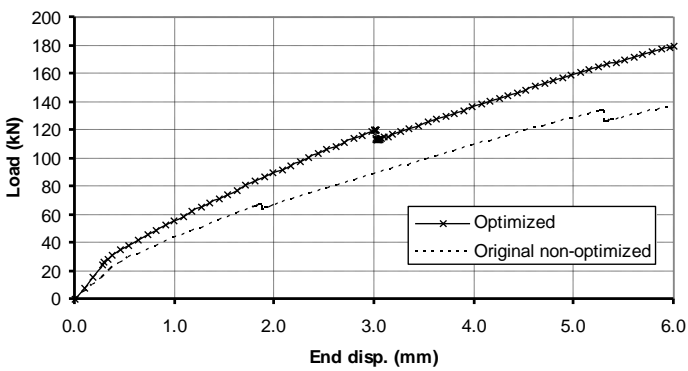


**Fig.7:** Numerical out-of-plane displacements in optimized composite plate.

## 7 Concluding remarks

The use of a simple technique to detect the onset of structural instabilities in a finite element analysis facilitated the development of a composite lay-up optimisation procedure to delay the onset of mode-jumping. Genetic Algorithms were also shown to be highly effective for this type of optimisation and the developed methodology is readily applicable to more complex composite structures.

## References

1. Falzon, B.G., The behaviour of damage tolerant hat-stiffened composite panels loaded in uniaxial compression. *Composites - Part A: Applied Science and Manufacturing*, Vol. 32, No. 9, pp. 1255-1262, 2001.
2. Falzon, B.G. and Steven, G.P., Postbuckling behaviour of hat-stiffened thin-skinned carbon-fibre composite panels. New Orleans, LA, USA, pp. 2663-2671, 1995.
3. Falzon, B.G. and Steven, G.P., Buckling mode transition in hat-stiffened composite panels loaded in uniaxial compression. *Composite Structures*, Vol. 37, No. 2, pp. 253-267, 1997.
4. Falzon, B.G. and Cerini, M., A study of secondary instabilities in postbuckling composite aerostructures. *The Aeronautical Journal*, Vol. No. pp. 715-729, November 2007.
5. Faggiani, A. and Falzon, B.G., Optimization strategy for minimising damage in postbuckling stiffened panels. *AIAA Journal*, Vol. 45, No. 10, pp. 2520-2528, 2007.
6. Koiter, W.T., Introduction to the post-buckling behaviour of flat plates. *Colloquium on the post-buckling behaviour of plates in metal structures*, University of Liege, pp. 1963.
7. ABAQUS/Implicit, Ver. 6.8, Dassault Systems, Providence, RI, 2008.
8. Falzon, B.G., Stevens, K.A., and Davies, G.O., Postbuckling behaviour of a blade-stiffened composite panel loaded in uniaxial compression. *Composites - Part A: Applied Science and Manufacturing*, Vol. 31, No. 5, pp. 459-468, 2000.
9. Noguchi, H. and Fujii, F., Eigenvector-free indicator, pinpointing and branch-switching for bifurcation. *Communications in Numerical Methods in Engineering*, Vol. 19, No. pp. 445-457, 2003.
10. Haftka, R.T. and Walsh, J.L., Stacking-sequence optimisation of laminated plates by integer programming. *AIAA Journal*, Vol. 30, No. 3, pp. 814-819, 1992.
11. Gurdal, Z., Haftka, R.T., and Hajela, P., *Design and optimisation of laminated composite materials* New York: Wiley. 1999.

### Copyright Statement

The authors confirm that they, and/or their company or organization, hold copyright on all of the original material included in this paper. The authors also confirm that they have obtained permission, from the copyright holder of any third party material included in this paper, to publish it as part of their paper. The authors confirm that they give permission, or have obtained permission from the copyright holder of this paper, for the publication and distribution of this paper as part of the ICAS2012 proceedings or as individual off-prints from the proceedings.